Am J Transl Res 2017;9(3):1183-1192
www.ajtr.org /ISSN:1943-8141/AJTR0037164

Original Article

GYY4137 stimulates osteoblastic cell proliferation and differentiation *via* an ERK1/2-dependent anti-oxidant mechanism

Meng Lv, Yang Liu, Ting-Hui Xiao, Wei Jiang, Bo-Wen Lin, Xiao-Ming Zhang, Yi-Miao Lin, Zhong-Shi Xu

Department of Orthopaedics, 2nd Clinical Medical College of Jinan University (Shenzhen People's Hospital), Shenzhen 518020, China

Received August 3, 2016; Accepted January 16, 2017; Epub March 15, 2017; Published March 30, 2017

Abstract: Objective: Oxidative stress plays a critical role in the development of osteoporosis. Hydrogen sulfide (H_2S), produces anti-oxidant effect in various biological systems. The present study found that GYY4137, a slow H_2S releasing compound, stimulated both mRNA level and activity of alkaline phosphatase, the marker of osteoblast differentiation. This research aims to explore the mechanism on how GYY4137 stimulates osteoblastic cell proliferation and differentiation via an ERK1/2-dependent anti-oxidant approach. Methods: The MC3T3-E1 osteoblast-like cell line was cultured in plate. After pretreatment with GYY4137 (100 μM) for 30 min, the cells were washed twice with PBS solution and then incubated in freshly prepared low serum medium containing 400 μM H_2O_2 for 4 h. Cells viability was evaluated with the MTT. Cell apoptosis was evaluated by the Hoechst 33342. Then, ALP activity, NO and the superoxide dismutase (SOD) activity is determined by assay kit accordingly, ALP mRNA is identified by RT-PCR. ERK1/2 was analyzed by Western blot. The ROS production was measured with a fluorescence reader. All data was analyzed by SPSS 16.0. Results: We found in the present study that GYY4137, a slow H_2S releasing compound, stimulated both mRNA level and activity of alkaline phosphatase, the marker of osteoblast differentiation. RT-PCR shows that GYY4137 stimulated the transcriptional levels of Runx2, a key transcription factor associated with osteoblast differentiation. These data suggest that GYY4137 may stimulate osteoblastic cell proliferation and differentiation. Moreover, GYY4137, which alone at 1-1000 μM had no significant effect, protected MC3T3-E1 osteoblastic cells against hydrogen peroxide (H_2O_2)-induced cell death and apoptosis. This was mediated by its anti-oxidant effect, as GYY4137 reversed the reduced superoxide dismutase activity and the elevated productions of reactive oxygen species and nitric oxide in the osteoblastic cells treated with H_2O_2. Western blotting analysis showed that the protective effects of GYY4137 were mediated by suppression of ERK1/2. Conclusions: GYY4137 stimulates osteoblastic cell proliferation and bone differentiation via an ERK1/2-dependent anti-oxidant mechanism. Our findings suggest that GYY4137 may have a potentially therapeutic value for osteoporosis.

Keywords: Oxidative stress, osteoporosis, bone formation, hydrogen sulfide, reactive oxygen species, ERK1/2

Introduction

Hydrogen sulfide (H_2S) has been positioned as the third gasotransmitter followed after nitric oxide (NO) and carbon monoxide (CO) [1]. It is synthesized by two pyridoxal-5'-phosphate dependent enzymes: cystathione-γ-lyase (CSE) and cystathione-β-synthase (CBS) [2], and one pyridoxal-5'-phosphate-independent enzyme 3-mercaptopyruvate sulfurtransferase (3-MST) [3]. H_2S concentration has been reported to be 2-5 μmol/L in human serum [4]. However, more recent estimates have indicated that the concentration of H_2S in brain or plasma may be much lower, which is in the nanomolar range. Ishigami *et al.* found that H_2S in brain is undetectable using gas chromatography, with a detection limit of 9.2 μM [5]. Furne *et al.* reported that free H_2S level in brain is approximately 14 nM by gas chromatography [6]. More importantly, H_2S has been found to produce multiple physiological and pathophysiological functions in various body systems [7-9]. One of the important biological functions of H_2S is anti-oxidative stress [10]. Since H_2S is a strong anti-oxidant reagent [11], the application of H_2S may decrease ROS level; and therefore, produce protective effects [12, 13].

Osteoporosis is an emerging medical and socioeconomic threat characterized by the systemic impairment of bone mass, strength, and microarchitecture [14, 15]. The decreased density of the bone weakens the bone and results in frequent bone fractures. Approximately 40% of postmenopausal women are affected by osteoporosis [16]. In an ageing population, this number is expected to steadily increase [17]. The osteoblast is a unique bone-forming cell derived from mesenchymal stem cells. The rate of bone formation is determined by the speed and effectiveness of precursor cells differentiating into mature osteoblasts, which secrete a bone matrix that can be mineralized within their life span. At sites of resorption lacunae, a team of osteoblasts produce an extracellular matrix containing type-1 collagen and various non-collagenous proteins, such as osteocalcin, osteonectin, osteopontin and others [18].

Bone formation can be suppressed by oxidative stress. There are markedly increased levels of various oxidative stress markers including reactive oxygen species (ROS) in blood [19]. For instance, in ovariectomized rats, a popular model of postmenopausal osteoporosis, levels of lipid peroxidation and H_2O_2 were found to be elevated while enzymatic antioxidants decreased in tissue homogenates from the femora [20]. We recently reported that H_2S may protect osteoblastic cells against oxidative stress [21]. The morpholin-4-ium 4 methoxyphenyl (morpholino) phosphinodithioate (GYY4137) is a novel water soluble donor of H_2S, which can release H_2S in slow, sustaining and more effective pattern. In this study, we investigated the effect of GYY4137 on H_2O_2-induced oxidative injury in MC3T3-E1 cells. We found that GYY4137 stimulated osteoblastic proliferation *via* an anti-oxidative mechanism. These data imply that GYY4137 may potentially be used to treat osteoporosis.

Material and methods

Cell culture

The murine calvaria-derived MC3T3-E1 osteoblast-like cell line (mouse C57BL/6 calvaria, subclone 4, ATCC No. 58078614) was purchased from the American Type Culture Collection (ATCC). Cells were seeded at 1×10^5 cells/ml into 75-cm^2 flasks, and maintained in minimum essential medium supplemented with 10% fetal bovine serum and 1% penicillin/streptomycin. The medium was replenished every three days. The medium was replenished every three days. Then, the cultures were induced to differentiate by transferring cells into a medium supplemented with L-ascorbic acid and β-glycerol phosphate at final concentrations of 50 μg/ml and 5 mM, respectively [22]. Cells were cultured at 37°C in a humidified atmosphere of 5% CO_2 and 95% O_2.

Cell treatment

Cells were seeded into 24-well plate and incubated until cells reach approximately 70% confluence. Regular medium was replaced with low-serum medium (0.5% FBS/α-MEM) immediately before the treatment. After pretreatment with GYY4137 for 30 min, cells were washed twice with PBS solution, and incubated in freshly prepared low-serum media containing different concentrations of H_2O_2 for four hours or otherwise stated. This treatment procedure excludes the possibility that GYY4137 directly reacts with H_2O_2.

Cell phenotypic observations were made using an Olympus DP50 inverted phase-contrast microscope, which was fitted with a digital camera system to capture images using the DP Soft software, monitor both the differentiation status of the cultures, and record any change during treatment.

Cell viability assay

Cell viability was evaluated using the MTT method, as previously described with modifications [23]. Cells were seeded in 96-well plate at approximately 1×10^5/well, and cultured overnight in an incubator. In brief, medium was aspirated at the end of the treatment, and 200 μl of fresh medium containing 0.5 mg/ml of MTT were added into all tested and control wells. After incubation at 37°C for four hours, the culture media containing MTT was removed. Then, DMSO (150 μl) was added into each well, and absorbance at 570 nm was measured using a spectrophotometric plate reader.

Quantification of apoptosis

In order to visualize nuclear morphology, cells were fixed in 4% paraformaldehyde and stained with 2.5 μg/ml of DNA dye Hoechst 33342.

Uniformly stained nuclei were scored as healthy, viable cells. Condensed or fragmented nuclei were scored as apoptotic. In order to obtain unbiased counting, the Petri dishes were coded, and cells were scored blindly without knowledge of their prior treatment.

Alkaline phosphatase (ALP) activity assay

The induction of ALP is an unequivocal marker for bone cell differentiation. In order to observe osteoblastic differentiation, α-MEM containing 10% FBS, antibiotics, 50 mg/ml of ascorbic acid, and 5 mM of ß-glycerophosphate (ß-GP) were used during treatment. In order to measure ALP activity, cells were seeded in a 12-well plate and treated with Krebs (control), GYY4137 (100 μM), H_2O_2 (400 μM) and GYY4137 + H_2O_2. After treatment for four hours, H_2O_2 was washed out with the fresh medium. After culture for three days, the medium was removed, and the cell monolayer was gently washed twice with PBS. Then, cells were lysed with cell lysis buffer (0.5 mL for a 35 mm dish) and centrifuged at 12,000 × g for 10 minutes. The resulting supernatant was used for the measurement of ALP activity and protein concentration with a commercially available ALP activity assay kit (Cell Biolabs, Inc. USA) and a BCA-protein assay kit (Bio-Rad), respectively. ALP activity was expressed as nmol/min/mg of protein.

Nitric oxide (NO) determination

Nitrite, an indicator of NO production, was measured in a cell-free culture supernatant of osteoblasts using a commercial kit (Promega, Madison, WI, USA). Briefly, after treatment with GYY4137 and/or H_2O_2 for four hours, 50-μl aliquots of cell culture medium from each dish were collected and mixed with 100 μl of Griess reagent (50 μL of 1% sulfanilamide + 50 μL of 0.1% naphthylethylenediamine dihydrochloride in 2.5% H_3PO_4) in a 96-well plate. This mixture was incubated in the dark at room temperature for 15 minutes. The absorbance of NO_2^- was read at 520 nm using a plate reader.

Determination of superoxide dismutases (SOD) activity

Cells were collected after treatment with GYY4137 and/or H_2O_2 for one hour, and cellular SOD activity was determined using a SOD assay kit (Catalog No. 706002; Cayman Chemical Company, USA), according to manufacturer's instructions. SOD activity was expressed as units/mg of protein.

Western blot analysis of extra cellular signal-regulated kinase (ERK1/2)

At the end of the treatment with H_2O_2 (400 μM, 15 minutes, according to the time course experiment [data no shown]) with or without GYY4137 (100 μM, 30 minutes pretreatment), cells were washed with chilled PBS solution twice and harvested for protein extraction with a previously described method. Protein concentrations were determined with a NanoDrop Spectrophotometer (ND-1000, NanoDrop technology). Equal amounts of protein samples were separated by electrophoresis using a 10% sodium dodecyl sulfate-polyacrylamide (SDS/PAGE) gel, and transferred onto a nitrocellulose membrane (Whatman®, Germany). After blocking in 10% milk with TBS-T buffer (10 mM of Tris-HCl, 120 mM of NaCl, 0.1% Tween-20, pH 7.4) at room temperature for one hour, the membrane was incubated with the respective primary antibody (1:1,000) at 4°C overnight. Then, membranes were washed three times in TBS-T buffer, incubated with 1:10,000 dilutions of horseradish peroxidase-conjugated (HRP) anti-rabbit IgG at 25°C for one hour, and washed three times in TBS-T. Visualization was carried out using ECL® (plus/advanced chemiluminescence) kit (GE healthcare, UK). The density of the bands on Western blots was quantified by Image J software.

RT-PCR

Cells were seeded in 6-well plate and cultured for 72 hours with α-MEM containing 10% FBS, antibiotics, 50 mg/ml of ascorbic acid, and 5 mM of ß-glycerophosphate (ß-GP). The cells were treated with GYY4137 (100 μM) for 30 minutes and incubated with H_2O_2 (400 μM) for four hour. The mRNA levels of ALP, Runx2, and glyceraldehyde-3-phosphate dehydrogenase (GAPDH) were determined by reverse transcription PCR using a QIAGEN one-step RT-PCR kit (Qiagen). In brief, MC3T3-E1 cells were harvested and homogenized using TRIzol reagent (Invtirogen Co., Carlsbad, CA), and total RNA was isolated using a FastPrepFP 120 Instrument (BIO 101 Inc., Vista, CA). cDNA was constructed from the total RNA using various specific primers (Runx-F: 5'-CTCAGTGATTTAGGGCGCATT-3'; Runx-R: 5'-AGGGGTAAGACTGGT-

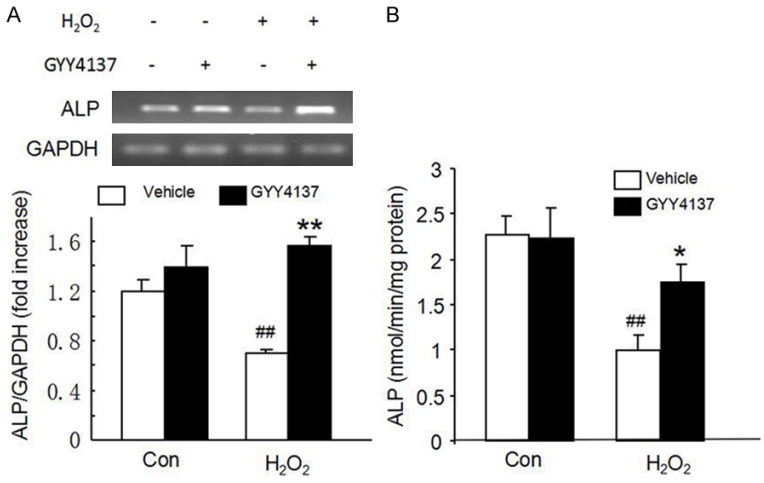

Figure 1. Effects of GYY4137 on the transcription and activity of ALP in MC3T3-E1 cells. A: Representative gel (upper panel) and mean data (lower panel) showing that GYY4137 attenuated H_2O_2 suppressed ALP mRNA level. B. GYY4137 ameliorated H_2O_2 (400 μM, 4 h) reduced ALP activity. n = 6. Mean ± S.E.M. *P < 0.05, **P < 0.01, ***P < 0.001 vs. the value of the group without GYY4137 treatment in the same group, #P < 0.05, ##P < 0.01, ###P < 0.001 vs. the corresponding values in the control group.

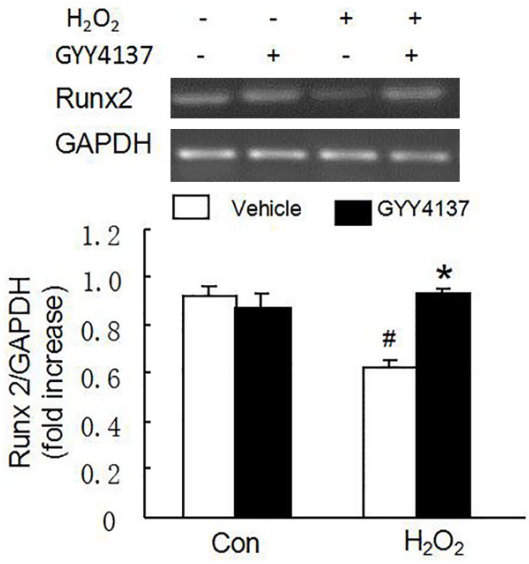

Figure 2. Effect of H_2S on Runx2 mRNA level. Representative gel (upper panel) and mean data (lower panel) showing that GYY4137 reversed H_2O_2 down-regulated Runx mRNA level. n = 3. Mean ± S.E.M. *P < 0.05 vs. the value without GYY4137 treatment in the H_2O_2 group; ##P < 0.01, ###P < 0.001 vs. the corresponding value in the control group.

CATAGG-3', ALP-F: 5'-CCATGGTAGATTACGCTCA-CA-3', ALP-R: 5'-ATGGAGGATTCCAGATACAGG3', GAPDH-F: ATCACCATCTTCCAGGAG-3', GAPDH-R: 5'-ATGGACTGTGGTCATGAG-3').

RT-PCR was conducted in a touchdown manner. Reverse transcription was performed at 56°C for eight minutes, 55°C for 10 minutes, 53°C for eight minutes, 51°C for eight minutes, 45°C for 10 minutes, and 95°C for 15 minutes. For polymerase chain reaction, one cycle of denaturation at 94°C for 20 seconds, annealing at 56°C for 20 seconds, and elongation at 72°C was performed. The annealing temperature was decreased by 1°C at each cycle. Finally, 33 cycles with an annealing temperature of 60.6°C (ALP, Runx2) and 57.6°C (GAPDH) were performed. PCR products were analyzed by 1% agarose gel electrophoresis and visualized by the Multigenius Bio-imaging system (Syngene, UK). In order to assess the level of gene transcription, the density of each band was normalized to the value of its corresponding housekeeping gene GAPDH.

ROS production

Cells were seeded in black 96-well plates and cultured for 48 hours. The culture medium was replaced with phenol red free DMEM containing H_2DCFDA (10 μM) 30 minutes before the treatment. Cells were treated with GYY4137 (100 μM) for 30 minutes. After being washed-out twice, cells were incubated with H_2O_2 (400 μM) for 30 minutes, one hour, or two hours. The ROS production was measured with a fluorescence reader (Safire2, Tecan Group Ltd.).

Chemicals and reagents

All chemicals were purchased from Sigma (Sigma, St. Louis, MO). Primary antibodies (anti-phospho- and anti-total-ERK1/2) were purchased from Cell Signaling (Beverly, MA, USA). The slow releasing H_2S donor morpholin-4-ium 4 methoxyphenyl phosphinodithioate (GYY4137) was synthesized, as previously described [24].

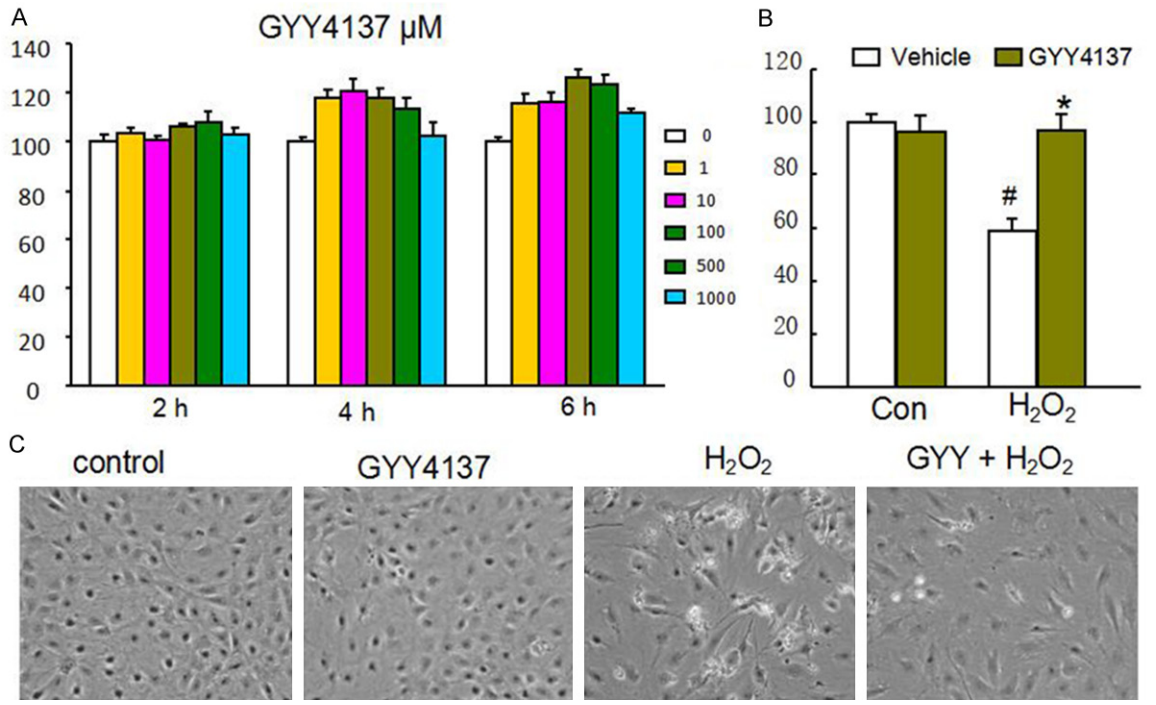

Figure 3. Protective effects of GYY4137 on H_2O_2-induced cell injury in MC3T3-E1 cells. A: Concentration and time dependent effects of GYY4137 on cell viability. GYY4137 (1-1000 μM) alone had no significant toxicity in MC3T3-E1 cells for up to 6 h. B: Pretreatment with GYY4137 (100 μM, 30 min) alleviated H_2O_2 (400 μM, 4 h)-induced cell injury. n = 6. Mean ± S.E.M. *P < 0.05 vs. the value without GYY4137 treatment in the H_2O_2 group; ##P < 0.01, ###P < 0.001 vs. the corresponding value in the control group. C: Morphological change of MC3T3-E1 osteoblastic cells incubated with GYY4137 or H_2O_2. Cells were treated with GYY4137 100 μM for 30 min before treatment with H_2O_2 400 μM for 4 h.

Statistical analysis

Data are expressed as means ± standard error of the mean (SEM). The difference between two groups was evaluated using Student's *t*-test. Multiple group comparison was performed using one-way analysis of variance followed by Turkey's post hoc test. A probability level of 0.05 was used to establish significance. All data was analyzed by SPSS 16.0.

Results

Effect of GYY4137 on the mRNA level and activity of ALP in MC3T3-E1 cells treated with H_2O_2

ALP is the earliest marker of osteoblast differentiation. Both mRNA level and activity of ALP were examined to evaluate the effect of GYY4137 on osteoblast differentiation. As shown in **Figure 1A**, the incubation of cells with H_2O_2 (400 μM) for four hours markedly reduced the mRNA level of ALP. GYY4137 significantly attenuated H_2O_2 and inhibited the transcriptional level of ALP. This was further supported by ALP activity. As shown in **Figure 1B**, treatment with H_2O_2 for four hours significantly decreased ALP activity in MC3T3-E1 cells after culture for three days. Cells pretreated with GYY4137 (100 μM) for 30 minutes abolished the effects of H_2O_2. Our data suggest that GYY4137 may stimulate osteoblast differentiation and proliferation.

Effect of GYY4137 on the gene expression of Runx-2 in MC3T3-E1 osteoblastic cells treated with H_2O_2

Runx-2 is a key transcription factor associated with osteoblast differentiation. As shown in **Figure 2**, treatment with H_2O_2 (400 μM) for four hours markedly reduced the mRNA level of Runx-2, which was significantly attenuated by GYY4137. These data suggests that GYY4137-activated osteoblast differentiation was mediated by Runx-2 stimulation.

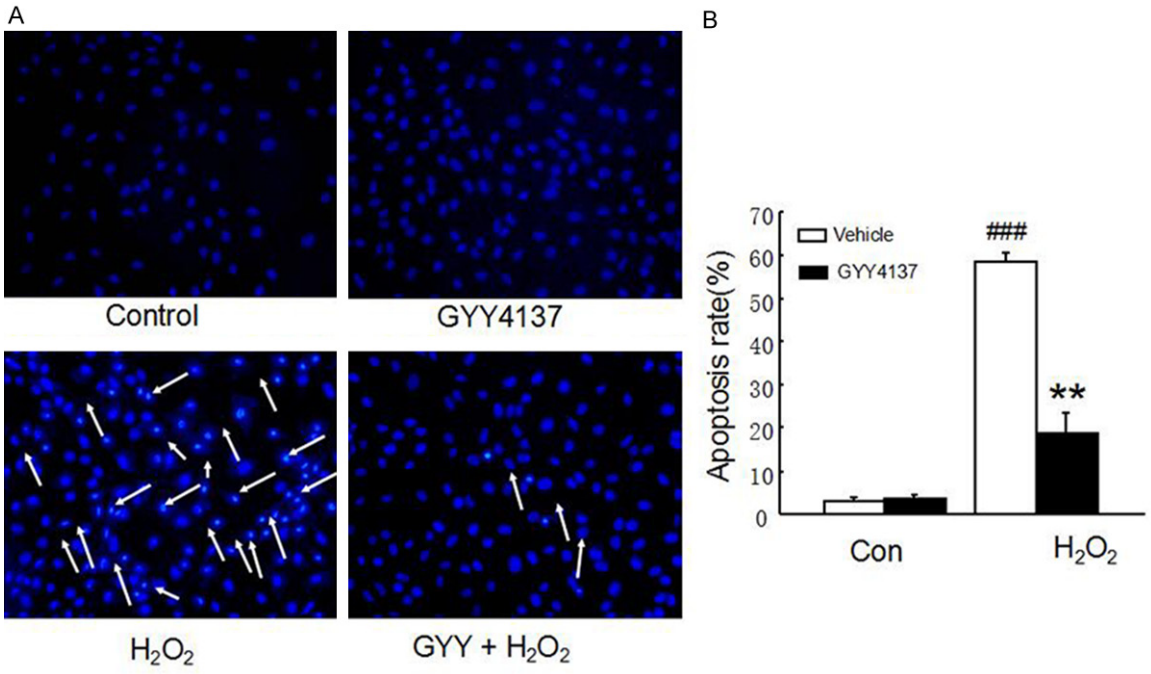

Figure 4. Effect of GYY4137 on H_2O_2-induced cell apoptosis in MC3T3-E1 cells. A: Cell apoptosis was detected by Hoechst 33342 staining in cells treated with vehicle, H_2O_2 (400 μM), H_2O_2 (400 μM) + GYY4137 (100 μM) and GYY4137 (100 μM) for 4 h. Arrows identify cells with condensed or fragmented nuclei, characteristic of apoptosis. B: Quantification of apoptosis based on nuclear condensation or fragmentation. Data were expressed as mean ± S.E.M. of three independent experiments. Mean ± S.E.M. *P < 0.05 vs. the value without GYY4137 treatment in the H_2O_2 group; ###P < 0.001 vs. the corresponding value in the control group.

GYY4137 protects H_2O_2-induced cell injury in MC3T3-E1 osteoblastic cells

The concentration-dependent and time-dependent effects of GYY4137 on cell viability were first investigated. As shown in **Figure 3A**, treatment with GYY4137 at a concentration range from 1 to 1,000 μM for 2-6 hours did not significantly affect the cell viability of MC3T3-E1 osteoblastic cells. However, treatment with H_2O_2 at 400 μM for four hours decreased cell viability. Pretreatment with GYY4137 (100 μM) for 30 minutes significantly protected MC3T3-E1 cells against H_2O_2-induced cell injury (**Figure 3B**).

The protective effect of GYY4137 was also confirmed by a morphological study. As shown in **Figure 3C**, H_2O_2 induced obvious morphological changes due to cell damage, as displayed by cell shrinkage and gradual detachment from culture dishes. Pretreatment with GYY4137 (100 μM) for 30 minutes dramatically alleviated H_2O_2-induced cell injury. These findings suggest that GYY4137 produces significant protection in MC3T3-E1 osteoblastic cells.

GYY4137 protects MC3T3-E1 cells against H_2O_2-induced cell apoptosis

Representative photomicrographs of the nuclei morphology of MC3T3-E1 cells are shown in **Figure 4**. Treatment with H_2O_2 (400 μM, four hours) induced a condensed and fragmented nuclei, which is a characteristic of apoptosis. Pretreatment with GYY4137 (100 μM, 30 minutes) significantly attenuated this effect. This confirms the protective effects of GYY4137 against H_2O_2-induced apoptosis in MC3T3-E1 cells.

Anti-oxidant effects of GYY4137 in osteoblastic cells

ROS release from MC3T3-E1 cells was also detected. As shown in **Figure 5A**, treatment with H_2O_2 (400 μM, four hours) significantly elevated ROS production. Pretreatment with GYY4137 (100 μM) for 30 minutes before the addition of H_2O_2 significantly attenuated the effect of H_2O_2 (**Figure 5A**). Similarly, H_2O_2 also stimulated the production of NO, a molecule considered as a precursor of a variety of reac-

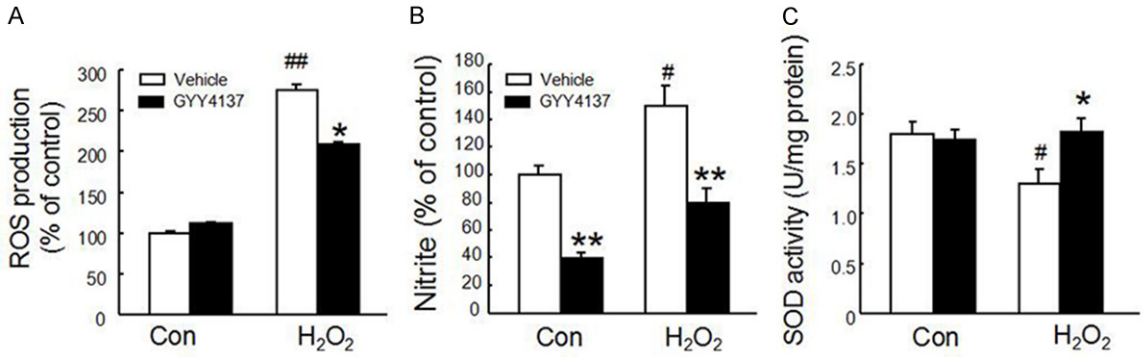

Figure 5. Effect of GYY4137 on the productions of ROS and NO and the activity of SOD in MC3T3-E1 cells. Pretreatement with GYY4137 (100 μM, 30 min) significantly suppressed the elevated productions of ROS release (A) and NO (B) and the suppressed SOD activity in cells treated with H_2O_2. n = 6. Mean ± S.E.M. *P < 0.05 vs. the value without GYY4137 treatment in the H_2O_2 group; ##P < 0.01, ###P < 0.001 vs. the corresponding values in the control group.

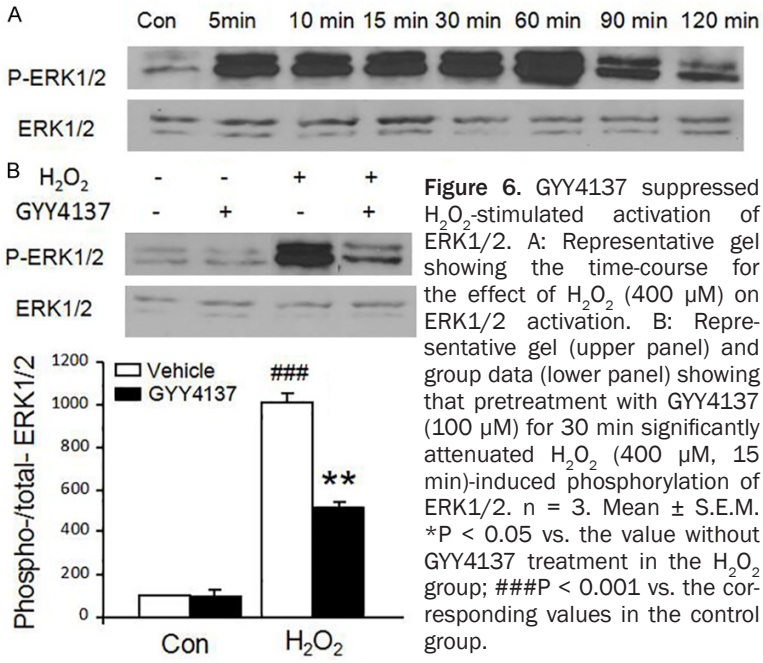

Figure 6. GYY4137 suppressed H_2O_2-stimulated activation of ERK1/2. A: Representative gel showing the time-course for the effect of H_2O_2 (400 μM) on ERK1/2 activation. B: Representative gel (upper panel) and group data (lower panel) showing that pretreatment with GYY4137 (100 μM) for 30 min significantly attenuated H_2O_2 (400 μM, 15 min)-induced phosphorylation of ERK1/2. n = 3. Mean ± S.E.M. *P < 0.05 vs. the value without GYY4137 treatment in the H_2O_2 group; ###P < 0.001 vs. the corresponding values in the control group.

tive nitrogen intermediates (**Figure 5B**). Pretreatment with GYY4137 abolished these effects.

The effect of GYY4137 was further determined on the activity of SOD, a ROS scavenger, in cells treated with H_2O_2. As shown in **Figure 5C**, H_2O_2 (400 μM) significantly suppressed SOD activity. GYY4137 (100 μM) significantly attenuated this effect, further confirming that GYY4137 may produce a significant anti-oxidative effect.

GYY4137 suppresses H_2O_2-stimulated ERK1/2 activation

In order to examine the involvement of ERK1/2, the time-course for H_2O_2-stimulated ERK1/2 activation was studied. As shown in **Figure 6A**, GYY4137 obviously stimulated ERK1/2 phosphorylation in as early as five minutes, which lasted for at least 90 minutes. **Figure 6B** shows that pretreatment with GYY4137 (100 μM) for 30 minutes significantly attenuated H_2O_2 (100 μM, 15 min)-induced ERK1/2 activation. These data suggest that H_2O_2-induced cell injury may involve the suppression of H_2O_2-induced ERK activation.

Discussion

The MC3T3-E1 osteoblastic cell line is a cell model commonly used in studying osteogenic development [25]. These cells are characterized by distinct proliferative and differentiated stages, thereby reproducing a temporal program consistent with osteoblast differentiation that occurs during *in vivo* bone formation [26]. In the present study, we observed that the protective effects of GYY4137 on osteoblastic proliferation and/or differentiation. ALP is a marker representing the osteoblast differentiation phenotype. We found that H_2O_2 significantly suppressed both the mRNA level and activity of ALP, which were reversed by GYY4137. These data suggests that GYY4137 may promote osteoblast proliferation and differentiation.

Skeletal development and bone remodeling require stringent control of gene activation and

suppression in response to physiological cues [27]. The fidelity of skeletal gene expression necessitates integrating a broad spectrum of regulatory signals that govern the commitment of osteoprogenitor and chondroprogenitor stem cells to bone cell lineage and the proliferation and differentiation of osteoblasts, as well as the maintenance of bone phenotype in osteocytes residing in a mineralized bone extracellular matrix. The requirements for the short-term developmental and sustained phenotypic expression of cell growth and bone-related genes are accommodated by the selective utilization of promoter regulatory elements. The extent to which genes are transcribed is determined by the temporal/spatial orchestration of combinatorial protein/DNA and protein/protein interactions that control the assembly, organization and activity of the regulatory machinery for physiological responsiveness. Runx/Cbfa/AML (runt homology domain) proteins play a pivotal role in governing the physiologically responsive control of skeletal genes. Aberrant expression of Runx proteins has been linked, in an obligatory manner, to perturbations in transcription and post-transcriptional regulation associated with developmentally compromised skeletogenesis and skeletal disease. Runx-2 is principally linked to osteoblast proliferation and differentiation, and is obligatory for the regulation of skeletal genes, hypertrophic chondrocytes, as well as endochondral and intramembraneous bone formation and skeletal development. For this reason, we measured the mRNA level of Runx-2 in the presence or absence of GYY4137 in MC3T3-E1 treated with H_2O_2. We found that GYY4137 significantly reversed the impact of H_2O_2 and suppressed the gene expression of Runx-2. These data suggest that GYY4137 may stimulate Runx-2 to stimulate osteoblast differentiation.

We further examined the effect of GYY4137 on cell morphology and viability in MC3T3-E1 cells treated with H_2O_2. We found that GYY4137 (100 μM) treatment for 30 min dramatically alleviated H_2O_2-induced cell damages, as displayed by cell shrinkage and gradual detachment from culture dishes. Cell viability analysis further confirmed that GYY4137 may protect osteoblastic cells against H_2O_2-induced cell injury.

Oxidative stress greatly contribute to the pathogenesis of various diseases including osteoporosis [28]. H_2O_2, one of the main ROS, may diffuse across biological membranes and produce a wide range of injury. It has been reported that H_2O_2 induces apoptosis or necrosis of various types of cells [29]. The fibronectin substratum damaged by ROS reduces the bone formation of osteoblastic cells *via* the inhibition of proliferation and/or differentiation of osteoblast progenitors, as well as the calcification process [30]. Therefore, reduced bone formation is commonly associated with increased oxidative stress in aged men and women [19]. A marked decrease in plasma antioxidants has also found in aged osteoporotic women [31].

Therefore, we further investigated whether the protective effects of GYY4137 is mediated by its anti-oxidant effect. We found that H_2O_2 significantly increased ROS production in MC3T3-E1 cells. As expected, GYY4137 significantly reduced ROS production in osteoblastic cells treated with H_2O_2. Oxidative stress also causes the release of NO. Similarly, we found that GYY4137 also significantly attenuated NO release in osteoblastic cells caused by H_2O_2. However, H_2S is a reducing agent. In this case, H_2S may scavenge ROS/H_2O_2 directly. This possibility can be excluded by the following reasons. First, unlike more abundant antioxidants (GSH present at 1-10 mM of concentration and Cys present at approximately 100 μM of concentration), H_2S is present at relatively low concentrations and is also a poor reductant (redox potential of +0.17 V *vs.* -0.25 V for the other two thiols) [32]. Hence, the physiological relevance of the antioxidant properties by itself remains an open question. Second, a similar protective effect was observed when GYY4137 or H_2S was removed before the addition of H_2O_2. This situation excludes the possibility that the anti-oxidant effect resulted from the direct scavenging of H_2O_2. These data imply that H_2S may induce a kind of "preconditioning" effect [33]. More importantly, it was found in the present study that GYY4137 suppressed H_2O_2-impaired SOD activity. The enhanced SOD activity by GYY4137 may scavenge excessive superoxide derived from oxidative damage, ameliorating H_2O_2-impaired cell survival and proliferation. These data suggest that the protective effects of GYY4137 were from its anti-oxidative action.

Previous studies have demonstrated that H_2O_2-induced apoptosis is mediated by the activa-

tion of ERK1/2 [34]. Activated MAPKs may phosphorylate their specific cascade proteins on serine and/or threonine residues [35], and thereby control many cellular events including cell proliferation, differentiation and cell death [36]. Therefore, we continued to study the underlying signaling mechanisms by examining the involvement of ERK1/2. Our results revealed that H_2O_2-stimulated ERK1/2 activation in as early as five minutes, and gradually diminished starting from 90 minutes. GYY4137, which alone had no significance, significantly attenuated the stimulatory effect of H_2O_2 on ERK1/2 activation. These data suggest that H_2S may protect osteoblasts by the suppression of ERK1/2 activity.

In conclusion, GYY4137 protects MC3T3-E1 cells against H_2O_2-impaired cell survival and proliferation. This is mediated by its anti-oxidant effect *via* an ERK1/2 dependent mechanism. Our results provide evidence that H_2S may have the potential therapeutic value to treat osteoporosis.

Acknowledgements

This work is supported by professor Jing-Song Bian from the National University of Singapore, he has an equal contribution.

Disclosure of conflict of interest

None.

Address correspondence to: Zhong-Shi Xu, Department of Orthopaedics, 2nd Clinical Medical College of Jinan University (Shenzhen People's Hospital), No. 1017 of Dongmen North Road, Luohu District, Shenzhen 518020, China. Tel: +86 755 25533018; Fax: +86 755 25533497; E-mail: zsxu_doc@163.com

References

[1] Wang R. Two's company, three's a crowd: can H_2S be the third endogenous gaseous transmitter? FASEB J 2002; 16: 1792-1798.

[2] Stipanuk MH and Beck PW. Characterization of the enzymic capacity for cysteine desulfhydration in liver and kidney of the rat. Biochem J 1982; 206: 267-277.

[3] Shibuya N, Tanaka M, Yoshida M,Ogasawara Y, Togawa T, Ishii K and Kimura H. 3-Mercaptopyruvate sulfurtransferase produces hydrogen sulfide and bound sulfane sulfur in the brain. Antioxid Redox Signal 2009; 11: 703-714.

[4] Jiang HL, Wu HC, Li ZL, Geng B and Tang CS. [Changes of the new gaseous transmitter H_2S in patients with coronary heart disease]. Di Yi Jun Yi Da Xue Xue Bao 2005; 25: 951-954.

[5] Ishigami M, Hiraki K, Umemura K, Ogasawara Y, Ishii K and Kimura H. A source of hydrogen sulfide and a mechanism of its release in the brain. Antioxid Redox Signal 2009; 11: 205-214.

[6] Furne J, Saeed A and Levitt MD. Whole tissue hydrogen sulfide concentrations are orders of magnitude lower than presently accepted values. Am J Physiol Regul Integr Comp Physiol 2008; 295: R1479-1485.

[7] Kimura H, Nagai Y, Umemura K and Kimura Y. Physiological roles of hydrogen sulfide: synaptic modulation, neuroprotection, and smooth muscle relaxation. Antioxid Redox Signal 2005; 7: 795-803.

[8] Li L, Bhatia M, Zhu YZ, Zhu YC, Ramnath RD, Wang ZJ, Anuar FB, Whiteman M, Salto-Tellez M and Moore PK. Hydrogen sulfide is a novel mediator of lipopolysaccharide-induced inflammation in the mouse. FASEB J 2005; 19: 1196-1198.

[9] Grassi F, Tyagi AM, Calvert JW, Gambari L, Walker LD, Yu M, Robinson J, Li JY, Lisignoli G, Vaccaro C, Adams J and Pacifici R. Hydrogen sulfide is a novel regulator of bone formation implicated in the bone loss induced by estrogen deficiency. J Bone Miner Res 2016; 31: 949-963.

[10] Gambari L, Lisignoli G, Cattini L, Manferdini C, Facchini A and Grassi F. Sodium hydrosulfide inhibits the differentiation of osteoclast progenitor cells via NRF2-dependent mechanism. Pharmacol Res 2014; 87: 99-112.

[11] Veeranki S and Tyagi SC. Role of hydrogen sulfide in skeletal muscle biology and metabolism. Nitric Oxide 2015; 46: 66-71.

[12] Whiteman M, Armstrong JS, Chu SH, Jia-Ling S, Wong BS, Cheung NS, Halliwell B and Moore PK. The novel neuromodulator hydrogen sulfide: an endogenous peroxynitrite 'scavenger'? J Neurochem 2004; 90: 765-768.

[13] Hu LF, Lu M, Hon Wong PT and Bian JS. Hydrogen sulfide: neurophysiology and neuropathology. Antioxid Redox Signal 2011; 15: 405-419.

[14] Lu YC, Lin YC, Lin YK, Liu YJ, Chang KH, Chieng PU and Chan WP. Prevalence of osteoporosis and low bone mass in older chinese population based on bone mineral density at multiple skeletal sites. Sci Rep 2016; 6: 25206.

[15] Aw D, Thain J, Ali A, Aung T, Chua WM, Sahota O, Weerasuriya N, Marshall L, Kearney F and Masud T. Predicting fracture risk in osteoporosis: the use of fracture prediction tools in an osteoporosis clinic population. Postgrad Med J 2016; 92: 267-270.

[16] Ma M, Chen X, Lu L, Yuan F, Zeng W, Luo S, Yin F and Cai J. Identification of crucial genes related to postmenopausal osteoporosis using gene expression profiling. Aging Clin Exp Res 2015; 28: 1067-1074.
[17] Burge R, Dawson-Hughes B, Solomon DH, Wong JB, King A and Tosteson A. Incidence and economic burden of osteoporosis-related fractures in the United States, 2005-2025. J Bone Miner Res 2007; 22: 465-475.
[18] Hu Y, Liu Y, Lajeunesse D, Mainard D, Jouzeau JY and Reboul P. Identification of two populations of osteoarthritic osteoblasts according to the 1,25[OH](2) vitamin D(3) potency to stimulate osteocalcin. Biomed Mater Eng 2015; 25 Suppl: 103-110.
[19] Basu S, Michaëlsson K, Olofsson H, Johansson S and Melhus H. Association between oxidative stress and bone mineral density. Biochem Biophys Res Commun 2001; 288: 275-279.
[20] Muthusami S, Ramachandran I, Muthusamy B, Vasudevan G, Prabhu V, Subramaniam V, Jagadeesan A and Narasimhan S. Ovariectomy induces oxidative stress and impairs bone antioxidant system in adult rats. Clin Chim Acta 2005; 360: 81-86.
[21] Xu ZS, Wang XY, Xiao DM, Hu LF, Lu M, Wu ZY and Bian JS. Hydrogen sulfide protects MC3T3-E1 osteoblastic cells against H_2O_2-induced oxidative damage-implications for the treatment of osteoporosis. Free Radic Biol Med 2011; 50: 1314-1323.
[22] Fatokun AA, Stone TW and Smith RA. Hydrogen peroxide-induced oxidative stress in MC3T3-E1 cells: the effects of glutamate and protection by purines. Bone 2006; 39: 542-551.
[23] Hu LF, Wang S, Shi XR and Hu G. ATP-sensitive potassium channel opener iptakalim protected against the cytotoxicity of MPP+ on SH-SY5Y cells by decreasing extracellular glutamate level. J Neurochem 2005; 94: 1570-1579.
[24] Whiteman M, Li L, Rose P, Tan CH, Parkinson DB and Moore PK. The effect of hydrogen sulfide donors on lipopolysaccharide-induced formation of inflammatory mediators in macrophages. Antioxid Redox Signal 2010; 12: 1147-1154.
[25] Fatokun AA, Stone TW and Smith RA. Responses of differentiated MC3T3-E1 osteoblast-like cells to reactive oxygen species. Eur J Pharmacol 2008; 587: 35-41.
[26] Quarles LD, Yohay DA, Lever LW, Caton R and Wenstrup RJ. Distinct proliferative and differentiated stages of murine MC3T3-E1 cells in culture: an in vitro model of osteoblast development. J Bone Miner Res 1992; 7: 683-692.
[27] Habig C, Geffers R and Distl O. A replication study for genome-wide gene expression levels in two layer lines elucidates differentially expressed genes of pathways involved in bone remodeling and immune responsiveness. PLoS One 2014; 9: e98350.
[28] Finkel T and Holbrook NJ. Oxidants, oxidative stress and the biology of ageing. Nature 2000; 408: 239-247.
[29] Gardner AM, Xu FH, Fady C, Jacoby FJ, Duffey DC, Tu Y and Lichtenstein A. Apoptotic vs. nonapoptotic cytotoxicity induced by hydrogen peroxide. Free Radic Biol Med 1997; 22: 73-83.
[30] Hosoya S, Suzuki H, Yamamoto M, Kobayashi K and Abiko Y. Alkaline phosphatase and type I collagen gene expressions were reduced by hydroxyl radical-treated fibronectin substratum. Mol Genet Metab 1998; 65: 31-34.
[31] Maggio D, Barabani M, Pierandrei M, Polidori MC, Catani M, Mecocci P, Senin U, Pacifici R and Cherubini A. Marked decrease in plasma antioxidants in aged osteoporotic women: results of a cross-sectional study. J Clin Endocrinol Metab 2003; 88: 1523-1527.
[32] Kabil O and Banerjee R. The redox biochemistry of hydrogen sulfide. J Biol Chem 2010; 285: 21903-21907.
[33] Bian JS, Yong QC, Pan TT, Feng ZN, Ali MY, Zhou S and Moore PK. Role of hydrogen sulfide in the cardioprotection caused by ischemic preconditioning in the rat heart and cardiac myocytes. J Pharmacol Exp Ther 2006; 316: 670-678.
[34] Park BG, Yoo CI, Kim HT, Kwon CH and Kim YK. Role of mitogen-activated protein kinases in hydrogen peroxide-induced cell death in osteoblastic cells. Toxicology 2005; 215: 115-125.
[35] Haddad JJ and Hanbali LB. Hypoxia upregulates MAPK(p38)/MAPK(ERK) phosphorylation in vitro: neuroimmunological differential time-dependent expression of MAPKs. Protein Pept Lett 2014; 21: 444-451.
[36] Davies SP, Reddy H, Caivano M and Cohen P. Specificity and mechanism of action of some commonly used protein kinase inhibitors. Biochem J 2000; 351: 95-105.